Circulation Research
JOURNAL OF THE AMERICAN HEART ASSOCIATION

American Heart Association®
Learn and Live℠

AMP-Activated Protein Kinase Functionally Phosphorylates Endothelial Nitric Oxide Synthase Ser633

Zhen Chen, I-Chen Peng, Wei Sun, Mei-I Su, Pang-Hung Hsu, Yi Fu, Yi Zhu, Kathryn DeFea, Songqin Pan, Ming-Daw Tsai and John Y-J. Shyy

Circ. Res. 2009;104;496-505; originally published online Jan 8, 2009;
DOI: 10.1161/CIRCRESAHA.108.187567
Circulation Research is published by the American Heart Association. 7272 Greenville Avenue, Dallas, TX 72514
 Print ISSN: 0009-7330. Online ISSN: 1524-4571

AMP-Activated Protein Kinase Functionally Phosphorylates Endothelial Nitric Oxide Synthase Ser633

Zhen Chen, I-Chen Peng, Wei Sun, Mei-I Su, Pang-Hung Hsu, Yi Fu, Yi Zhu, Kathryn DeFea, Songqin Pan, Ming-Daw Tsai, John Y-J. Shyy

Abstract—Endothelial nitric oxide synthase (eNOS) plays a central role in maintaining cardiovascular homeostasis by controlling NO bioavailability. The activity of eNOS in vascular endothelial cells (ECs) largely depends on posttranslational modifications, including phosphorylation. Because the activity of AMP-activated protein kinase (AMPK) in ECs can be increased by multiple cardiovascular events, we studied the phosphorylation of eNOS Ser633 by AMPK and examined its functional relevance in the mouse models. Shear stress, atorvastatin, and adiponectin all increased AMPK Thr172 and eNOS Ser633 phosphorylations, which were abolished if AMPK was pharmacologically inhibited or genetically ablated. The constitutively active form of AMPK or an AMPK agonist caused a sustained Ser633 phosphorylation. Expression of gain-/loss-of-function eNOS mutants revealed that Ser633 phosphorylation is important for NO production. The aorta of AMPK$\alpha 2^{-/-}$ mice showed attenuated atorvastatin-induced eNOS phosphorylation. Nano–liquid chromatography/tandem mass spectrometry (LC/MS/MS) confirmed that eNOS Ser633 was able to compete with Ser1177 or acetyl-coenzyme A carboxylase Ser79 for AMPKα phosphorylation. Nano-LC/MS/MS confirmed that eNOS purified from AICAR-treated ECs was phosphorylated at both Ser633 and Ser1177. Our results indicate that AMPK phosphorylation of eNOS Ser633 is a functional signaling event for NO bioavailability in ECs. **(*Circ Res*. 2009;104:496-505.)**

Key Words: AMPK ■ eNOS ■ endothelial cells ■ nitric oxide bioavailability ■ phosphorylation

The endothelium is pivotal in the regulation of vascular tone, which largely depends on endothelial nitric oxide synthase (eNOS)-derived NO bioavailability.[1–3] In addition to relaxing vessels, NO exerts such pleiotropic effects as anti-inflammation and antithrombosis on the vascular wall.[4,5] Existing as a homodimer, eNOS contains an N-terminal oxygenase domain, an interposed Ca^{2+}/calmodulin (CaM) binding domain, and a C-terminal reductase domain.[6] Much progress has been made in understanding the regulatory mechanisms of eNOS at transcriptional, translational, and posttranslational levels. The phosphorylation/dephosphorylation of Ser and Thr of eNOS by protein kinases/phosphatases seems to be important for its enzymatic activity in vascular endothelial cells (ECs).[7]

To date, 5 Ser/Thr phosphorylation sites in eNOS have been identified. They are Ser114, Thr495, Ser615, Ser633, and Ser1177 in human and mouse eNOS, which correspond to Ser116, Thr497, Ser617, Ser635, and Ser1179 in the bovine counterpart.[8] Functioning as stimulatory phosphorylation sites, Ser633 and Ser1177 are located in each of the 2 autoinhibitory sequences (ie, AIS I and II).[9–11] The phosphorylation of Ser1177 appears to eliminate the blockage of electron transfer within the C termini of the 2 eNOS monomers.[12] The phosphorylation of Ser1177 has been suggested to be critical for eNOS activation responding to several stimuli, such as shear stress, adiponectin, and 3-hydroxy-3-methylglutaryl-coenzyme A (HMG-CoA) inhibitors (ie, statins), known to increase NO bioavailability.[13–15] These physiological and pharmacological stimuli activate a number of protein kinases, including AMP-activated protein kinase (AMPK), protein kinase (PK)A, PKB (Akt), CaM-dependant protein kinase (CaMK)II, and PKG, which in turn phosphorylate Ser1177.[9,13,16–21] The Ser633 residue in eNOS resides in the flavin mononucleotide binding domain.[11] The gain-of-function phosphomimetic eNOS Ser635D mutant yielded increased basal and vascular endothelial growth factor– or ATP-stimulated NO release in transfected COS-7 cells.[10] Such experiments suggested that Ser633 might be more efficacious than Ser1177 in augmenting the eNOS-derived NO bioavailability. Furthermore, phosphorylation of Ser633 may enhance NO production without changing the intracellular calcium level ($[Ca^{2+}]_i$),[22] and it seems to be a later event

Original received May 25, 2008; resubmission received September 16, 2008; revised resubmission received December 19, 2008; accepted December 30, 2008.

From the Division of Biomedical Sciences (Z.C., I.-C.P., W.S., Y.F., K.D., J.Y.-J.S.), Biochemistry and Molecular Biology Graduate Program (I.-C.P.,), and W. M. Keck Proteomics Laboratory (S.P.), Institute for Integrative Genome Biology, University of California, Riverside; Department of Physiology and Pathophysiology (Y.F., Y.Z.), Health Science Center, Peking University, Beijing, China; and Genomics Research Center (M.-I.S., P.-H.H., M.-D.T.) and Institute of Biological Chemistry (M.-D.T.), Academia Sinica, Taipei, Taiwan.

Correspondence to John Y.-J. Shyy, PhD, Division of Biomedical Sciences, University of California, Riverside, CA 92521. E-mail john.shyy@ucr.edu

Circulation Research **is available at http://circres.ahajournals.org** **DOI: 10.1161/CIRCRESAHA.108.187567**

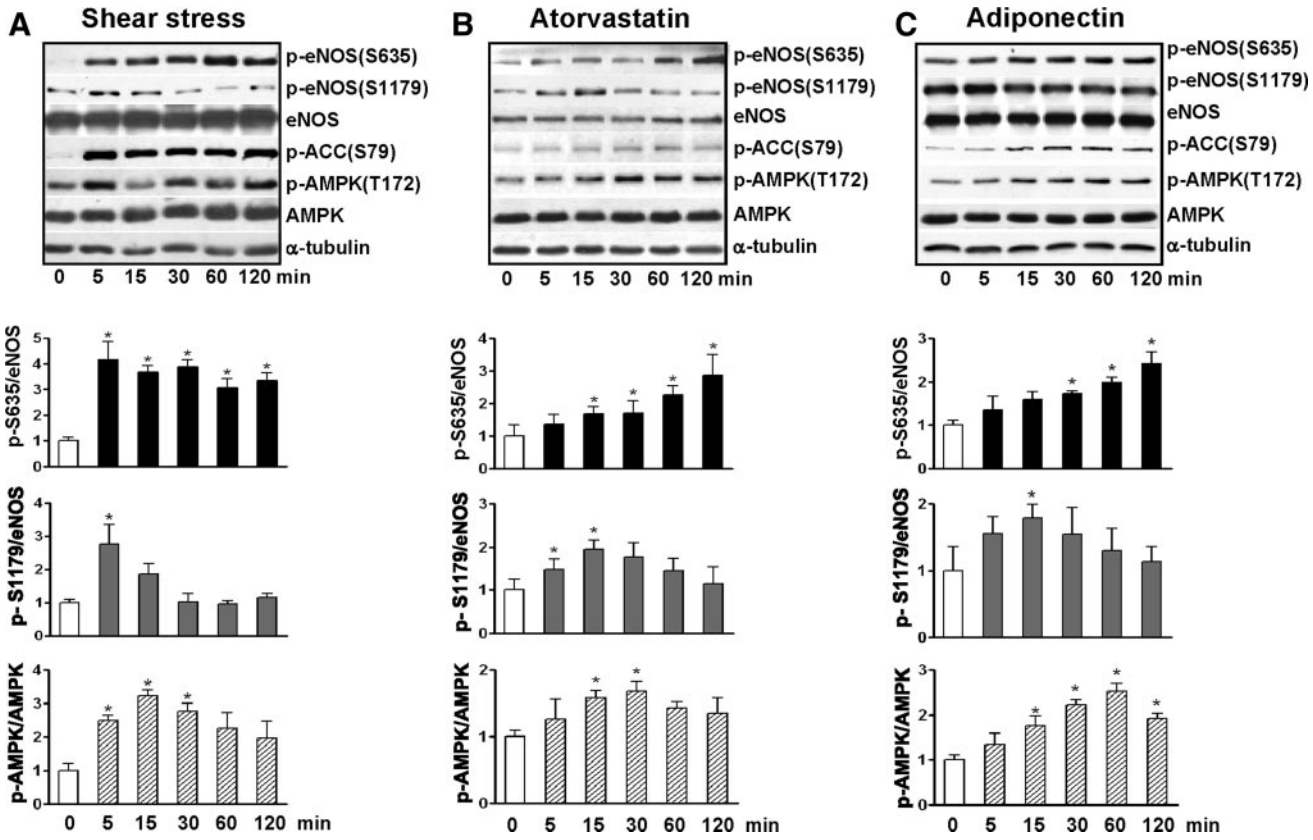

Figure 1. Shear stress, statin, and adiponectin enhance phosphorylation of AMPK Thr172 and eNOS Ser635 in BAECs. Confluent monolayers of BAECs were preexposed to laminar shear stress at 5 dyn/cm^2 for 6 hours, which was increased to 12 dyn/cm^2 for the durations shown (A), treated with atorvastatin at 1 μmol/L (B), or adiponectin at 30 μg/mL (C) for the indicated times. The cells were then lysed and underwent SDS-PAGE, followed by Western blotting with various primary antibodies. The bar graphs below are densitometry quantifications of the ratios of phospho-eNOS at Ser635 or Ser1179 to total eNOS and that of phospho-AMPK Thr172 to total AMPKα. The data are means±SD from 3 independent experiments, with static cells (A) or untreated controls (B and C) set as 1. *$P<0.05$ compared to control groups.

than that of Ser1177.[23] Thus, this posttranslational modification of Ser633 is proposed to maintain persistent eNOS activity after its initial activation by calcium flux. Using the PKA inhibitors H89 and PKI, Boo et al suggested that PKA, rather than Akt, phosphorylates Ser633 in ECs subjected to shear stress.[23]

AMPK is an energy sensor/metabolic switch, because AMPK phosphorylates and hence regulates the activity of enzymes such as acetyl-CoA carboxylase (ACC) and HMG-CoA reductase.[24,25] AMPK consists of a catalytic α subunit and regulatory β and γ subunits. The different isoforms of the subunits of AMPK are encoded by distinct genes (α1, α2, β1, β2, γ1, γ2, and γ3) and expressed differentially depending on tissue types.[26] Substantial evidence demonstrates that AMPK is not only critical in regulating metabolic homeostasis but also important in cardiovascular biology, attributable in part to AMPK-activating eNOS in ECs and cardiomyocytes.[27–29] By far, the activation of eNOS by AMPK is thought to be mediated through the phosphorylation of Ser1177 under many physiological conditions and pharmacological stimuli.[16,17,30,31]

Despite the plausible role of Ser633 phosphorylation contributing to eNOS-derived NO activity, the functional basis of this phosphorylation event is largely unknown. In this study, we addressed whether AMPK is an upstream kinase that phosphorylates Ser633, whether Ser633 competes with ACC Ser79 and eNOS Ser1177 for catalysis by AMPKα, and whether Ser633 phosphorylation is required for NO bioavailability.

Materials and Methods

The resources of antibodies and reagents, as well as detailed methods for cell culture, fluid shear stress experiments, adenoviral infection, small interfering (si)RNA knockdown, Western blotting, kinase activity assays, and NO bioavailability assays are described in expanded Materials and Methods section in the online data supplement, available at http://circres.ahajournals.org.

Animal Experiments

The animal experimental protocols were approved by the University of California at Riverside Institutional Animal Care and Use Committee. C57BL6 mice were purchased from The Jackson Laboratory. AMPK$\alpha2^{-/-}$ mice were originally created by Dr B. Viollet.[32] Atorvastatin at 50 mg/kg body weight was administered to male mice (8 weeks old) by gastric gavage. Saline was fed to control mice as a vehicle control. After 6, 12, or 24 hours, mice were killed, and abdominal aortas were removed. Proteins from aortic extracts were resolved by 8% SDS-PAGE and underwent Western blotting analysis.

SAMS, eNOS633, and eNOS1177 Binding Assays

eNOS633 and eNOS1177 peptides were synthesized with the sequences PLVSSWRRKRKESSNTDSA and RTQEVTSRIRTQSFS-

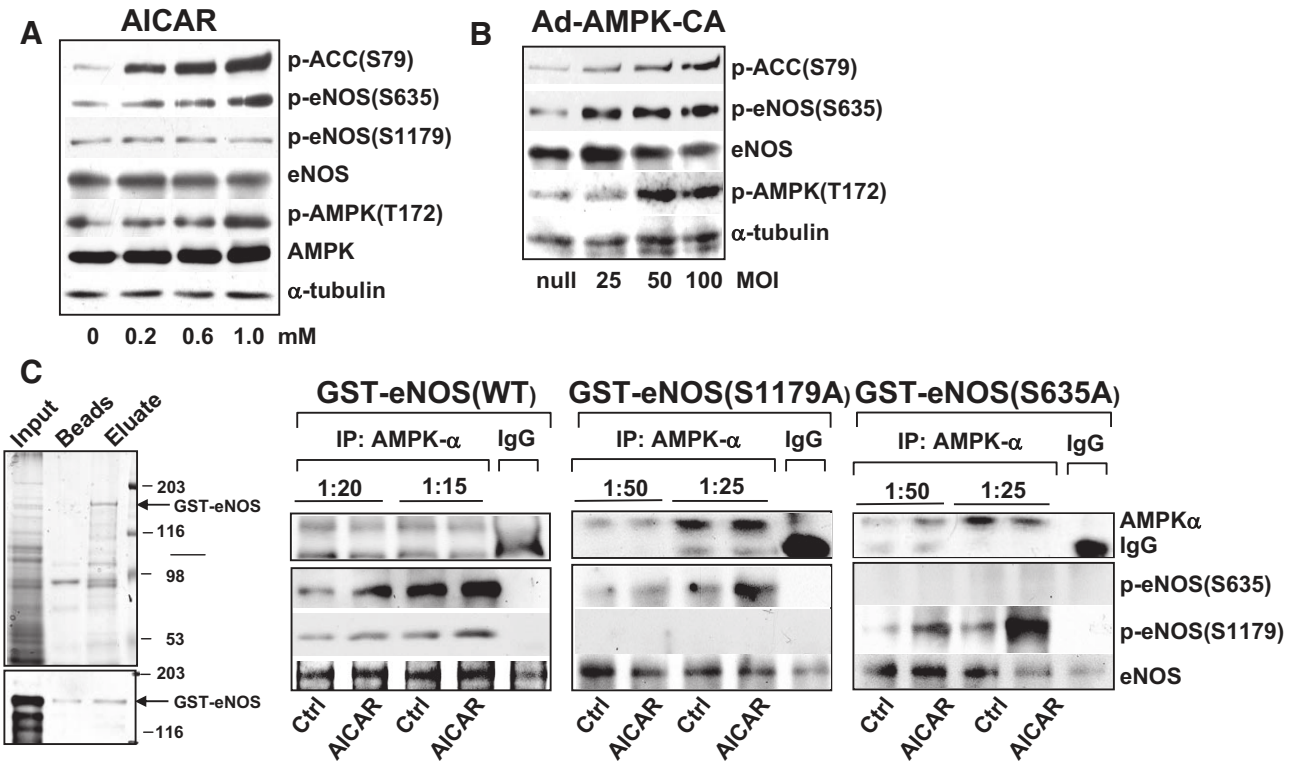

Figure 2. AMPK phosphorylates eNOS Ser635 in cultured ECs. Confluent BAECs were treated with various concentrations of AICAR for 15 minutes (A) or infected with Ad-AMPK-CA at different multiplicities of infection (MOI) for 24 hours (B). The control cells were infected with Ad-null virus at 50 multiplicities of infection. Cell lysates were analyzed by Western blotting with the indicated antibodies. C, BAECs were treated with AICAR at 1 mmol/L for 15 minutes or left untreated as controls. AMPKα was immunoprecipitated from cell lysates with the use of anti–pan-AMPKα at 1:20 or 1:15 dilution. Rabbit IgG was used as an IP control. The kinase activity of immunoprecipitated AMPKα was assayed with recombinant GST-eNOS (wild type [WT]), GST-eNOS (S1179A), or GST-eNOS (S635A) as substrates. Left, The expressed GST-eNOS is shown by Coomassie blue staining and Western blotting. The phosphorylation of GST-eNOS S1179 and S635 by the immunoprecipitated AMPKα was detected by Western blotting. The level of immunoprecipitated AMPKα and GST-eNOS used in the assays was also shown by immunoblotting. Data represent results from 3 independent experiments.

LQER, respectively. Bovine aortic endothelial cells (BAECs) were treated with AICAR for 30 minutes, and AMPK was immunoprecipitated. The phosphorylation of SAMS, eNOS633, and eNOS1177 peptides by AMPK was determined by the incorporation of ^{32}P. The kinase assays were performed in 40 mmol/L HEPES, 0.2 mmol/L AMP, 8 μCi (γ-^{32}P) ATP, 0.2 mmol/L ATP, 80 mmol/L NaCl, 5 mmol/L $MgCl_2$, 8% glycerol, and 0.8 mmol/L dithiothreitol at 37°C for 1 hour. The reaction mixture was spotted onto Whatman P81 filter paper and washed 5 times with 1% phosphoric acid and once with acetone. After being air-dried, the ^{32}P incorporation was quantified by use of a Beckman liquid scintillation counter.

Nano–Liquid Chromatography/Mass Spectrometry

For all liquid chromatography/mass spectrometric (LC/MS) and LC/tandem MS (LC/MS/MS) experiments, the Waters' nano-Acquity UPLC (ultra performance liquid chromatography) and Q-TOF Premier mass spectrometer were used (Waters, Milford, Mass). The detailed procedures of LC/MS and LC/MS/MS are described in the supplemental methods.

Statistical Analysis

The significance of variability was determined by Student's *t* test or 1-way ANOVA. All results are presented as means±SD from at least 3 independent experiments. In all cases, $P<0.05$ was considered statistically significant.

Results

AMPK and eNOS Ser635 Phosphorylation in Cultured ECs

AMPK is activated by several physiological and pharmacological stimuli such as shear stress, statins, and adiponectin, and is associated with eNOS phosphorylation at Ser1177/1179.[17,30,33] We examined first the effect of these stimuli on phosphorylation of eNOS Ser633/635 in cultured ECs. BAECs were treated with laminar flow, atorvastatin, or recombinant adiponectin for up to 2 hours. As shown in Figure 1, these 3 stimuli increased the phosphorylation of eNOS Ser635 as early as 5 minutes, which was sustained for up to 2 hours. The sustainable increase in phosphorylation was also observed for AMPK Thr172 and its target ACC Ser79. However, the phosphorylation of eNOS Ser1179 was increased only transiently in response to these stimuli, reaching a peak level at 5 or 15 minutes and declining afterward.

AMPK Phosphorylates Both eNOS Ser635 and Ser1179 In Vitro

The temporal phosphorylation of eNOS Ser635 and AMPK Thr172 as seen in Figure 1 suggests that eNOS Ser635 may be a catalytic target of AMPK. To test whether AMPK can phosphorylate eNOS Ser635, we treated BAECs with

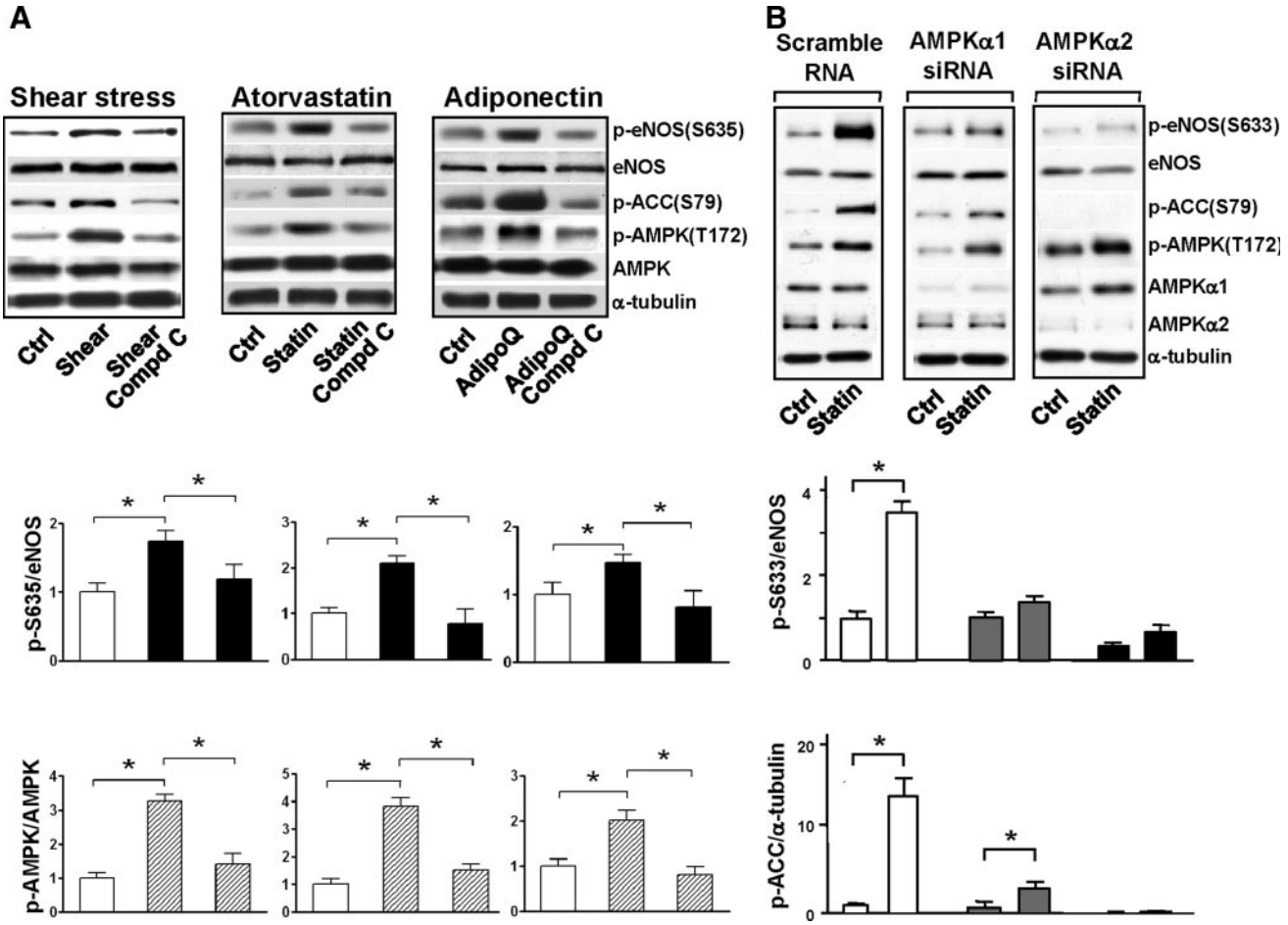

Figure 3. AMPK inhibition attenuates eNOS Ser635 phosphorylation in ECs. A, BAECs were pretreated with compound C at 20 μmol/L for 30 minutes before undergoing 30-minute treatment with laminar shear stress at 12 dyn/cm^2, atorvastatin at 1 μmol/L, or adiponectin at 30 μg/mL. In B, HUVECs were transfected with AMPKα1 siRNA, AMPKα2 siRNA, or scramble RNA (10 nmol/L) before atorvastatin treatment. Phosphorylation of eNOS Ser635, AMPK Thr172, and ACC Ser79 was revealed by Western blotting. The bar graphs represent the densitometry analyses of Western blotting as means±SD of 3 or 4 independent experiments. *$P<0.05$ between groups as indicated.

AICAR, an AMPK-specific agonist, or infected BAECs with Ad-AMPK-CA, an adenoviral vector expressing the constitutively active form of AMPK. AICAR treatment increased the phosphorylation of eNOS at both Ser635 and Ser1179 in a dose-dependent manner (Figure 2A and the online data supplement, Figure I, A). Similarly, Ad-AMPK-CA infection increased phosphorylation of eNOS Ser635 in ECs, as compared with Ad-null infection in control cells (Figure 2B and supplemental Figure I, B).

Using immunoprecipitation (IP) kinase activity assay, we examined next whether AMPK can directly phosphorylate eNOS Ser635. As shown in Figure 2C, AMPKα immunoprecipitated from AICAR-stimulated BAECs phosphorylated glutathione *S*-transferase (GST)-eNOS at both Ser635 and Ser1179, as revealed by Western blot analysis. Phosphorylation was elevated with increased concentration of AMPK antibody used for IP. GST-eNOS with S/A mutation at either Ser635 or Ser1179 was used in parallel assays. As expected, phosphorylation by AMPK at the mutated site was abolished, but the other site was unaffected. Collectively, these results suggest that AMPK can directly and specifically phosphorylate eNOS at Ser635.

To determine whether AMPK is necessary for eNOS Ser635 phosphorylation, BAECs were treated with compound C, an AMPK antagonist, before treatment with laminar flow, atorvastatin, or recombinant adiponectin. As shown in Figure 3A, AMPK and ACC phosphorylation was impaired in ECs treated with compound C, as compared with that in control cells. With AMPK inhibited by compound C, the phosphorylation of eNOS Ser635 by laminar flow, atorvastatin, or adiponectin was also greatly attenuated, which suggests that AMPK is required for eNOS Ser635 phosphorylation. We used siRNA to knock down AMPKα1 or -α2 in human umbilical vein endothelial cells (HUVECs). The isoform-specific AMPK knockdown by siRNA also decreased eNOS Ser633 phosphorylation caused by atorvastatin (Figure 3B).

AMPK Activation Mediates eNOS Ser633 Phosphorylation In Vivo

To correlate the in vitro findings in Figures 1 through 3 with in vivo conditions, we explored whether AMPK regulates eNOS phosphorylation at Ser633 (rodent and human homolog of bovine eNOS Ser635) in the mouse

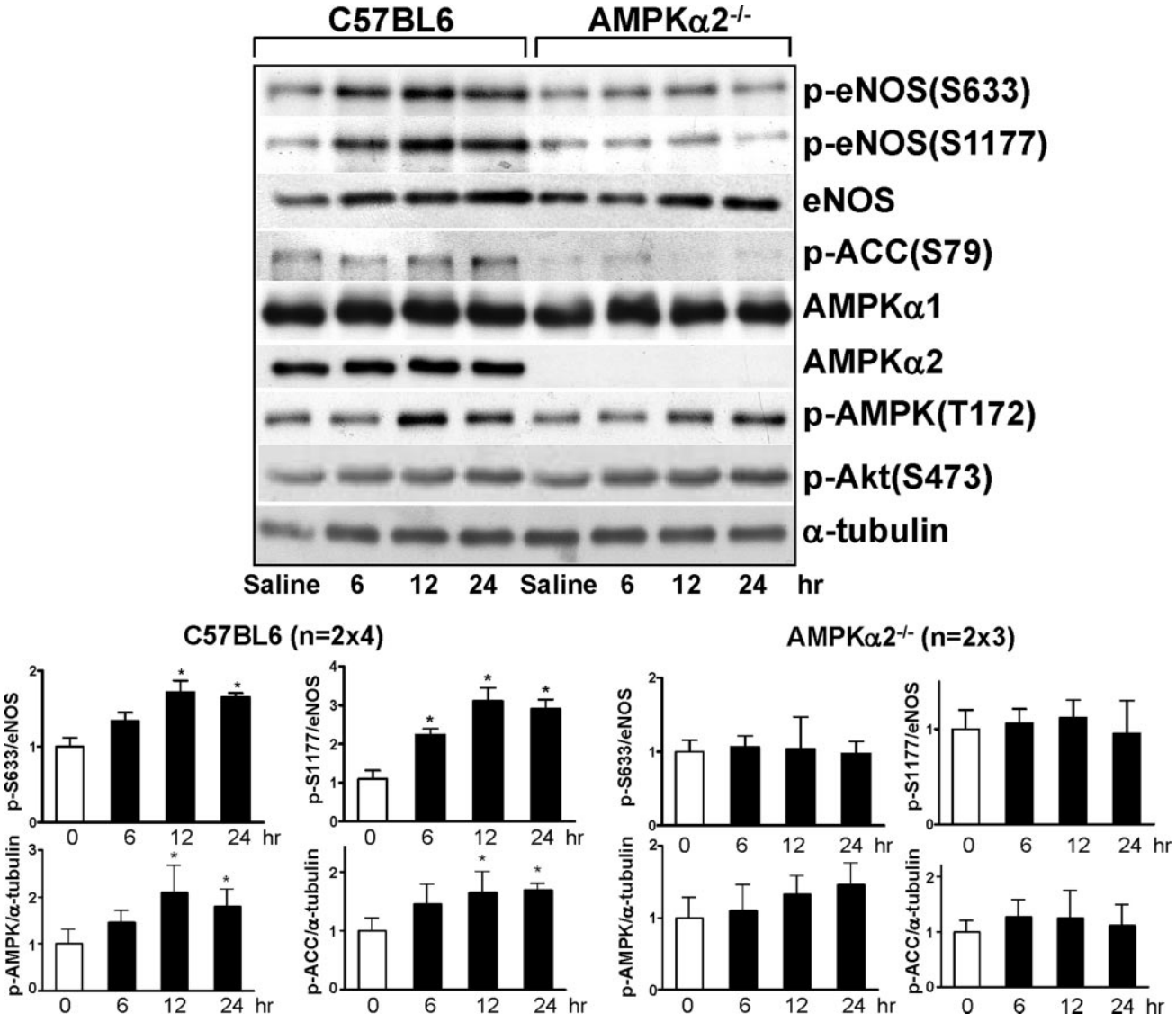

Figure 4. AMPK mediates eNOS Ser633 phosphorylation in mouse aortas in vivo. C57BL6 (A) or AMPK$\alpha 2^{-/-}$ (B) mice were given atorvastatin at 50 mg/kg body weight for the indicated times before euthanasia. In the control group, mice received the same volume (0.5 mL) of saline 6 hours before euthanasia. Tissue extracts from 2 aortas were pooled into 1 sample to be analyzed by Western blotting with various antibodies as indicated. The bar graphs are results of densitometry analyses of the ratio of phospho-eNOS to total eNOS, phospho-AMPK, and phosphor-ACC to α-tubulin. The saline controls were set as 1. Data represent means±SD from 3 independent experiments. *$P<0.05$ between atorvastatin-treated and control mice.

vessel wall. C57BL6 wild-type mice were given atorvastatin (50 mg/kg body weight), and eNOS phosphorylation in the aorta was analyzed. Consistent with the results obtained in vitro, AMPK Thr172 phosphorylation in vivo was increased by atorvastatin for up to 24 hour, a pattern similar to that for phosphorylation of eNOS Ser633 (Figure 4).

In contrast, AMPK and ACC phosphorylation in aortas of AMPK$\alpha 2^{-/-}$ mice treated with atorvastatin increased marginally. Furthermore, the phosphorylation levels of eNOS Ser633 and Ser1177 in AMPK$\alpha 2^{-/-}$ mice were noticeably lower than those in the C57BL6 wild-type mice, with atorvastatin. However, Akt Ser473 phosphorylation still increased with atorvastatin administration in AMPK$\alpha 2^{-/-}$ mice (Figure 4).

NO Production Caused by AMPK Phosphorylation of eNOS Ser635

NO assays were performed to test the functional relevance of AMPK phosphorylating eNOS Ser633/635. Because HEK293 cells express AMPKα1 and α2 but not eNOS (Z.C. and J.Y.-J.S., unpublished results, 2008), we transfected these cells with plasmids encoding the wild-type eNOS, 635A, or 635A1179A mutants. The cells were then treated with AICAR to activate AMPK. HEK293 cells were also transfected with phospho-mimetic eNOS mutants 635D or 635D1179D. In eNOS-expressing (wild-type) cells treated with AICAR, the level of NO was elevated, similar to cells infected with Ad-AMPK-CA (Figure 5A). A comparable level of NO production was observed in cells transfected with 635D or 635D1179D. In contrast, NO production was low in

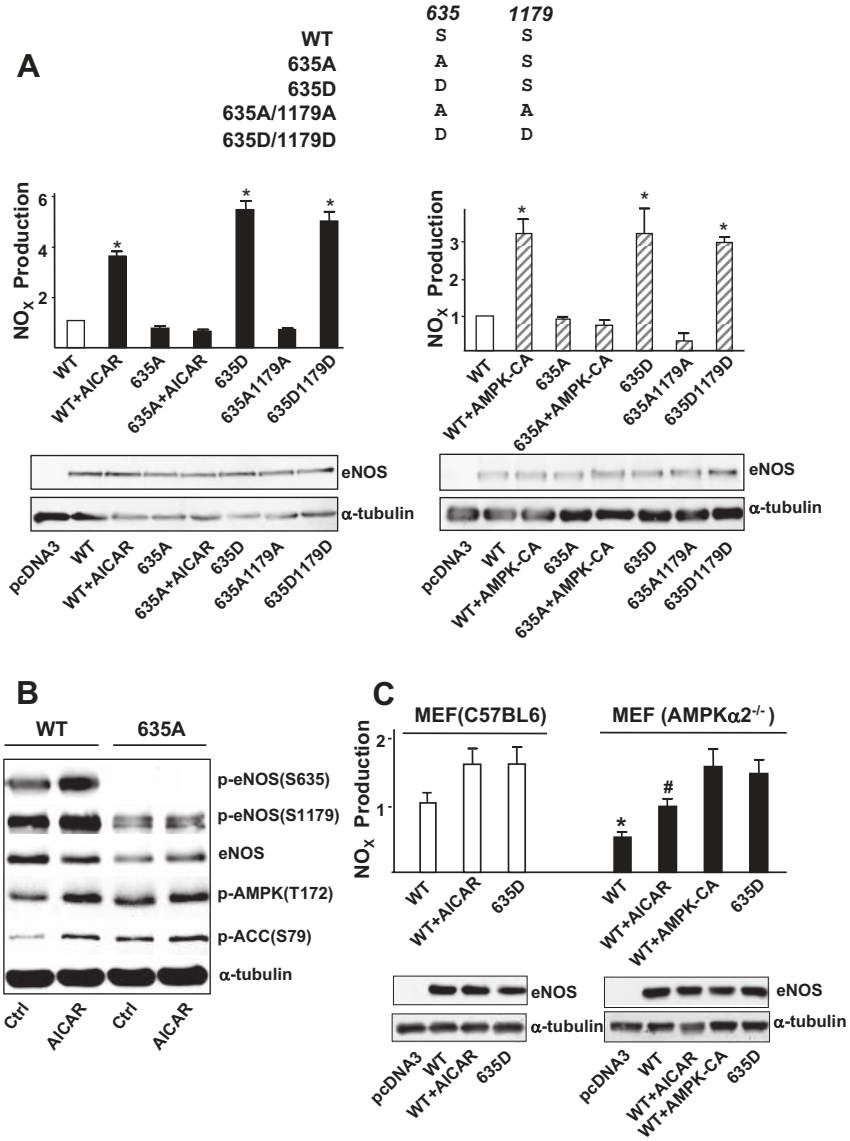

Figure 5. AMPK is necessary for eNOS S635-mediated NO bioavailability. A, HEK293 cells were transfected with various plasmids expressing the wild-type (WT) and mutated eNOS (ie, 635A, 635D, 635A/1179A, and 635D/1179D). One set of cells transfected with WT or 635A was treated with AICAR (1 mmol/L), and in parallel experiments, another set was infected with Ad-AMPKα2-CA (100 multiplicities of infection). The NO bioavailability from various cells was determined by Griess assay and expressed as NO_x. In all experiments, the NO_x produced from cells transfected with pcDNA3 was considered background and thus subtracted from total NO_x values of all cell groups. On Western blotting, the relative level of expressed eNOS was normalized to that of α-tubulin. NO_x production was further normalized to the relative level of eNOS. B, HEK293 cells transfected with WT or 635A eNOS were treated with AICAR (1 mmol/L) for 15 minutes. Cell lysates were resolved on SDS-PAGE and subjected to Western blotting with various antibodies as indicated. C, MEFs isolated from C57BL6 or AMPK$\alpha 2^{-/-}$ mice were transfected with various eNOS plasmids in the presence or absence of AICAR or coinfected with Ad-AMPK-CA, as indicated. NO_x production was measured accordingly. In A, NO_x produced from HEK293 cells transfected with WT-eNOS was set as 1. In C, NO_x value corresponding to C57BL6 MEFs transfected with WT-eNOS was set as 1. Data are means±SD from 5 independent experiments. In A, *$P<0.05$ compared with HEK293 cells transfected with WT eNOS. In C, *$P<0.05$ between C57BL6 MEFs and AMPK$\alpha 2^{-/-}$ MEFs transfected with WT-eNOS; #$P<0.05$ between C57BL6 MEFs and AMPK$\alpha 2^{-/-}$ MEFs transfected with WT-eNOS and then treated with AICAR.

cells expressing eNOS 635A or 635A1179A, which mimicked dephosphorylation, with AICAR treatment or with Ad-AMPK-CA infection. The phosphorylation of eNOS Ser635 and Ser1179 was increased in cells treated with AICAR (Figure 5B). Phospho-eNOS (S635) antibody could not detect any phosphorylation event in cells transfected with eNOS 635A, which was consistent with the low production of NO. We also compared NO production in murine embryonic fibroblasts (MEFs) isolated from C57BL6 and AMPK$\alpha 2^{-/-}$ embryos. As shown in Figure 5C, the ablation of AMPKα2 resulted in impaired NO bioavailability in MEFs expressing eNOS (wild type), at the basal level and under AICAR stimulation. The NO production level was similar in C57BL6 and AMPK$\alpha 2^{-/-}$ MEFs transfected with 635D. In addition, supplementing AMPK$\alpha 2^{-/-}$ MEFs with Ad-AMPK-CA restored the NO production to the level of that in cells expressing 635D. Taken together, these results suggest that AMPK regulates eNOS function, at least in part, through phosphorylating eNOS Ser633/635.

AMPK Shows Comparable Activities Toward eNOS Ser633/635 and Ser1177/1179

Because AMPKα could phosphorylate eNOS Ser633/635, Ser1177/1179, and ACC Ser79, we hypothesized that the 3 substrates might share the same catalytic site(s) within AMPKα, and, therefore, they might be mutually exclusive and compete each other for phosphorylation. To test this, we used synthetic peptides instead of full-length proteins for the kinase activity and substrate competition assays.

Two synthetic peptides with sequences flanking human eNOS S633 and S1177 (Figure 6A), respectively, showed a phosphorylation level similar to that of SAMS, an ACC homology (Figure 6B). To verify that the 3 peptides bind to the same active site of AMPK with comparable affinities, we performed nano-LC/MS analysis to test the competition between SAMS, S633, and S1177 peptides for AMPKα phosphorylation. The expected mass and *m*/*z* are shown in supplemental Table I. A mixture of SAMS and S1177 peptide was included in the AMPKα IP kinase assays. Nano-LC/MS

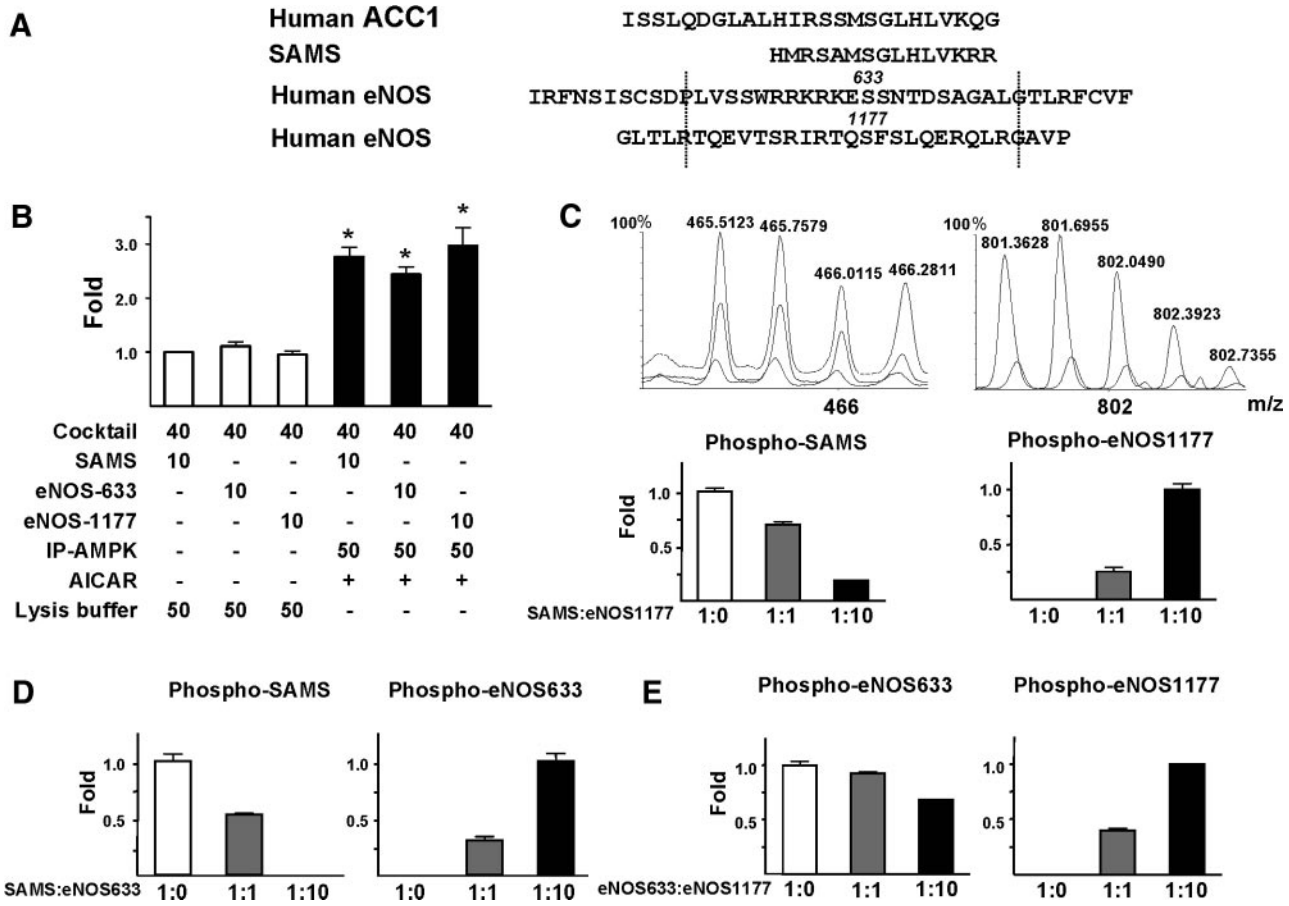

Figure 6. Competition between eNOS Ser633/635 and Ser1177/1179 for AMPK phosphorylation detected by LC/MS. Shown in A are peptide sequences of SAMS and those adjacent to human ACC1 Ser79, human eNOS Ser633, and human eNOS Ser1177. The sequences shown indicate the synthesized S633 and S1177 oligopeptides. B, BAECs were treated with AICAR (1 mmol/L) for 15 minutes and lysed. AMPK was immunoprecipitated from BAEC lysates by anti–pan-AMPKα. SAMS, S633, or S1177 (1 mmol/L) together with (γ-^{32}P) ATP (8 μCi) were mixed with the immunoprecipitated AMPKα for IP kinase activity assays. The phosphorylation of SAMS, S633, and S1177 peptides was determined by the incorporation of ^{32}P. The scintillation counts of various samples were normalized to that of control containing reaction cocktail (40 μL), SAMS (10 μL), and lysis buffer (50 μL) set as 1. *$P<0.05$ compared with control. C, SAMS and S1177 peptides were mixed at ratios of 1:0, 1:1, and 1:10, and the peptide mixture was included in AMPKα IP kinase assays. Nano-LC/MS was performed to detect the phosphorylated SAMS and S1177. The spectra show *m/z* around 466 and 802, with the dashed, solid, and dotted lines representing SAMS: S1177 at 1:0, 1:1, and 1:10, respectively. Phosphorylated SAMS and eNOS633 peptides were detected as positive ions with *m/z* 465.49, 4+, and *m/z* 571.79, 4+, respectively. Quantitation of signal intensity for individual ions was based on the maximal apex–peak height (ie, ion counts) displayed on the *m/z* spectrum derived from summing all individual scans across the entire retention time of the corresponding ion on the extracted ion chromatogram. The baseline background was subtracted from the above peak height to obtain extracted ion total counts (EITC), which was then used to quantify the changes of phosphorylation level for each peptide, with the highest value set as 1. Data are means±SD from triplicate experiments. Similar analyses were performed to assess the competition between SAMS and S633 (D) or that between S633 and S1177 (E) for AMPKα phosphorylation.

revealed that the phosphorylation of SAMS and S1177 depended on the ratios of peptide mixed (Figure 6C). A similar competition between SAMS and S633 was found (Figure 6D). Furthermore, peptides S633 and S1177 mutually competed with each other for AMPKα (Figure 6E).

Although LC/MS analysis indicated that both S633 and S1177 peptides were phosphorylated by AMPK, the exact amino acids were undetermined. To further elucidate whether Ser633/635 phosphorylation is physiologically relevant, we immunoprecipitated eNOS from AICAR-treated BAECs for nano-LC/MS/MS analysis. As shown in Figure 7, phosphorylation of eNOS Ser635 and Ser1179 indeed occurred concurrently in ECs with activated AMPK. The phosphorylated Ser within the corresponding tryptic peptides was shown by characteristic neutral loss of the phosphate group (H_3PO_4), which reduced the mass value of Ser from 87 to 69 Da. This result, together with that from peptide competition assay, suggests that Ser633 and Ser1177 are comparable AMPK substrates in ECs.

Discussion

Shear stress, statins, and adiponectin are physiological, pharmacological, and hormonal stimuli that are beneficial for NO bioavailability. All 3 of these stimuli exert positive effects on the phosphorylation of AMPK Thr172 and eNOS Ser633/635. In complementary experiments, genetic or pharmacological inhibition of AMPK attenuated phosphorylation of eNOS Ser633/635, with attendant decrease in NO production. IP kinase assay was previously used to reveal the phosphorylation of Ser1177/1179 by Akt.[9,13] Here, we used a similar

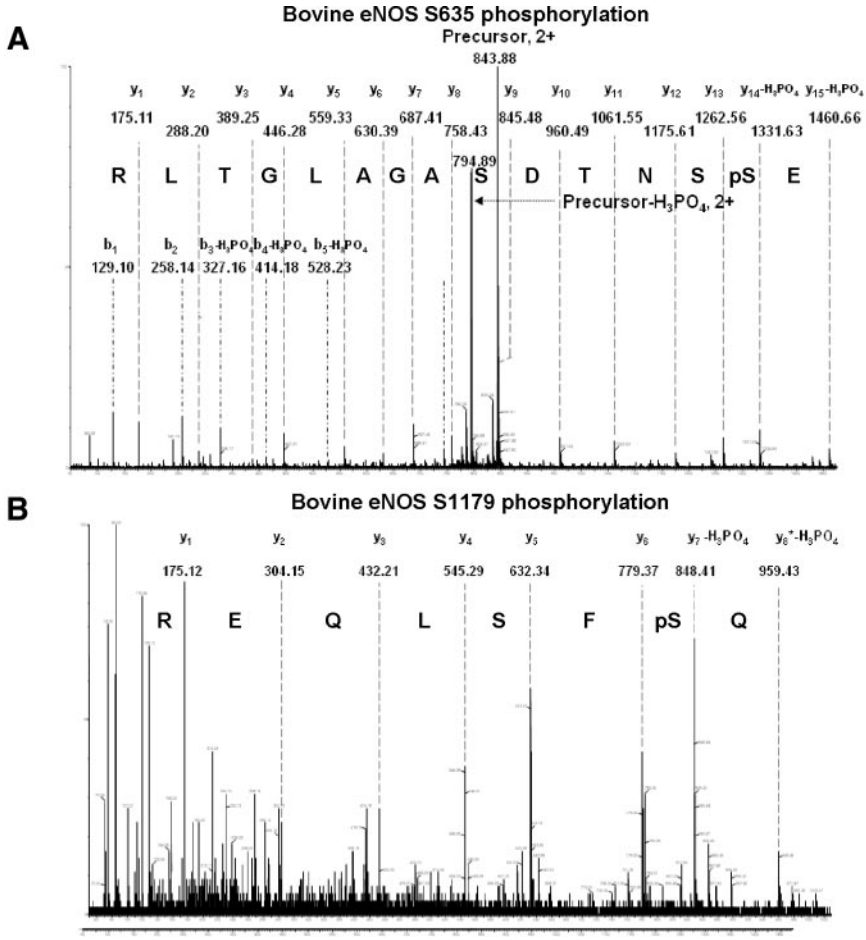

Figure 7. LC/MS/MS analysis of eNOS Ser635 and Ser1179 phosphorylation in BAECs. eNOS immunoprecipitated from AICAR-treated BAECs was trypsin-digested and then passed through TiO_2-coated magnetic beads to enrich phosphopeptides. Nano-LC/MS/MS was used to map the phosphorylation site within the peptides containing Ser635 (A) or Ser1179 (B).

approach to demonstrate that Ser633/635 is a direct target site of AMPKα. The hierarchy of AMPK in phosphorylating eNOS Ser633 in vivo was confirmed in AMPK$\alpha 2^{-/-}$ mice receiving atorvastatin. Because endothelium-dependent vessel dilation is mainly regulated by eNOS-mediated NO release, our data suggest that AMPK-eNOS Ser633/635 is a major signaling pathway for endothelial biology.

The phosphorylation of Ser633/635 and Ser1177/1179 is stimulatory for eNOS activity with increased NO production.[10] The phosphorylation of Ser635 was more sustained than that of Ser1179 in BAECs, regardless of type of stimulation (Figure 1). Among the 4 putative "gain-of-function" eNOS mutants (ie, S116D, S617D, S635D, and S1179D), eNOS S635D was the most efficacious in enhancing NO production.[10] Figure 5 indicates that NO production with this mutant was similar to that with 635D1179D, which suggests a possible redundancy of Ser1179 phosphorylation in regulating NO production. Structurally, Ser633/635 may be phosphorylated once Ser1177/1179 is phosphorylated and hence removes the hindrance imposed by AIS II, where Ser1177/1179 resides.[34] IP kinase assay (Figure 2C) showed that Ala mutation of Ser1177/1179 or Ser633/635 did not affect the AMPK phosphorylation of either. This finding seems inconsistent with previous observations of Ser1179 phosphorylation level unchanged with Ser635 mutated to Ala, whereas Ser635 phosphorylation was increased with Ser1179 mutated to Ala.[10] This discrepancy might be caused by distinct protein folding of GST-eNOS and endogenous eNOS in living cells.

Several other kinases are implicated in phosphorylating eNOS Ser633/635 and Ser1177/1179. PKA, but not Akt, was suggested to phosphorylate eNOS Ser633/635.[11,15,19] However, PKA, Akt, and CaMKII have been suggested to phosphorylate Ser1177/1179.[18,19,9,13,20] One major experimental approach in these previous studies was the use of various kinase inhibitors. For example, H89, a PKA inhibitor, when used at 10 μmol/L, also suppressed the AMPK kinase activity by 80%.[35] We found statin-induced ACC Ser79 phosphorylation impaired in ECs pretreated with H89 at 10 μmol/L (data not shown). The use of Ad-Akt-DN, H89, KN-93 (a CaMKII inhibitor), and PKA siRNA did not inhibit the shear stress–induced phosphorylation of AMPK Thr172 or eNOS Ser633/635 (supplemental Figures II and III). Although the atorvastatin-induced eNOS Ser633 phosphorylation was much attenuated in aortas of AMPK$\alpha 2^{-/-}$ mice, the level of Akt Ser473 phosphorylation, an indication of Akt activity, remained high (Figure 4). The α1 of AMPK seems to be the major isoform in the endothelium.[36] However, knocking out α2 was sufficient to reduce the ACC and eNOS phosphorylation in the ECs and mouse aorta (Figures 3B and 4). These results are consistent with a previous finding that the AMPKα2 subunit is more important than α1 in

MEFs for the activation of AMPK by hypoxia or glucose deprivation.[37] Previous study by Kemp and colleagues indicated that $\beta 1$ is crucial for the assembly of AMPK heterotrimer.[38] Apparently, the aortic expression of $\beta 1$ was slightly affected by the ablation of $\alpha 2$ (data not shown). Thus, the AMPK trimeric complexes consisting of $\alpha 1\beta 1$ in AMPK$\alpha 2^{-/-}$ mice did not seem to exert compensatory activity to phosphorylate eNOS Ser633.

The SAMS peptide is a modified version of the 15 amino acids flanking ACC Ser79. AMPK phosphorylates SAMS peptide with a K_m of 30 ± 2 μmol/L and V_{max} of 8.1 ± 1.5 μmol/min per milligram,[39,40] which is $\approx$2.5 times higher than that of ACC. A peptide encompassing HMG-CoA reductase Ser871, the putative AMPKα phosphorylating site, had a K_m of 22 ± 4 μmol/L.[41] A 16-aa peptide containing eNOS Ser1177 was phosphorylated by AMPK, with a K_m of 54 ± 6 μmol/L and V_{max} of 5.8 ± 0.3 μmol/min per milligram.[16] We showed that each of the 19-aa eNOS peptides (ie, S633 and S1177) could compete with SAMS for AMPKα phosphorylation, and the competition occurred at similar concentrations of the peptides. Thus, AMPKα would phosphorylate eNOS Ser633/635, eNOS Ser1177/1179, ACC Ser79, and HMG-CoA reductase Ser871 with comparable enzyme kinetics. Such comparability has physiological implications. ACC and HMG-CoA reductase, the rate-limiting enzymes for fatty acid and cholesterol synthesis, are ubiquitously expressed in almost all cell types. Depending on cellular energy level and the ensuing AMPK activation status, ACC, HMG-CoA reductase, and other enzymes involved in metabolism are phosphorylated to regulate energy storage/mobilization. However, eNOS expression is highly restricted to endothelial cells and cardiomyocytes, where NO bioavailability is imperative.[42] AMPK phosphorylates ACC, HMG-CoA reductase, and other AMPK targets in cells where eNOS expression is limited, thereby controlling lipid metabolism. In cardiovascular cells, where eNOS is abundant, eNOS and ACC are competitive substrates for AMPK. Not only energy balance (eg, lipid synthesis) but also eNOS-mediated NO bioavailability is thus regulated by AMPK in these cells.

The similar enzyme kinetics among eNOS 633, eNOS 1177, HMG-CoA reductase, and SAMS peptides suggests that eNOS, HMG-CoA reductase, and ACC may compete for the same catalytic site(s) of AMPKα. LC/MS/MS analysis showed that both eNOS Ser633 and Ser1177 are phosphorylated in AICAR-treated cells (Figure 7). Scott et al suggested that a pseudosubstrate sequence, conserved in the eukaryotic AMPKγ, binds to the catalytic groove of AMPKα when AMP does not bind to the γ subunit.[43] Because of the resemblance between the peptide sequence of the pseudosubstrate and those flanking AMPK target sites, including ACC Ser79, HMG-CoA reductase Ser871, and eNOS Ser1177, an AMPK consensus recognition motif ($\approx$22 aa) was thereby proposed.[44] Interestingly, the deduced hydrophobic and basic residues that are important for AMPK recognition align similarly with those between eNOS Ile616 and Asp637.

In conclusion, this study suggests that AMPKα is the primary kinase phosphorylating eNOS Ser633/635, which is functionally linked to NO bioavailability. The functional and kinetic information reported herein should be useful for future investigation of the structure–function relationship of AMPK catalysis in endothelial biology.

Sources of Funding

This study was supported in part by NIH grants HL77448 and HL89940 (to J.Y.-J.S.).

Disclosures

None.

References

1. Furchgott RF, Zawadzki JV. The obligatory role of endothelial cells in the relaxation of arterial smooth muscle by acetylcholine. *Nature*. 1980;288:373–376.
2. Palmer RM, Ferrige AG, Moncada S. Nitric oxide release accounts for the biological activity of endothelium-derived relaxing factor. *Nature*. 1987;327:524–526.
3. Stuehr DJ. Mammalian nitric oxide synthases. *Biochim Biophys Acta*. 1999;1411:217–230.
4. Lerman A, Zeiher AM. Endothelial function: cardiac events. *Circulation*. 2005;111:363–368.
5. Loscalzo J. Nitric oxide insufficiency, platelet activation, and arterial thrombosis. *Circ Res*. 2001;88:756–762.
6. Andrew PJ, Mayer B. Enzymatic function of nitric oxide synthases. *Cardiovasc Res*. 1999;43:521–531.
7. Sessa WC. eNOS at a glance. *J Cell Sci*. 2004;117:2427–2429.
8. Mount PF, Kemp BE, Power DA. Regulation of endothelial and myocardial NO synthesis by multi-site eNOS phosphorylation. *J Mol Cell Cardiol*. 2007;42:271–279.
9. Fulton D, Gratton JP, McCabe TJ, Fontana J, Fujio Y, Walsh K, Franke TF, Papapetropoulos A, Sessa WC. Regulation of endothelium-derived nitric oxide production by the protein kinase Akt. *Nature*. 1999;399:597–601.
10. Bauer PM, Fulton D, Boo YC, Sorescu GP, Kemp BE, Jo H, Sessa WC. Compensatory phosphorylation and protein-protein interactions revealed by loss of function and gain of function mutants of multiple serine phosphorylation sites in endothelial nitric-oxide synthase. *J Biol Chem*. 2003;278:14841–14849.
11. Michell BJ, Harris MB, Chen ZP, Ju H, Venema VJ, Blackstone MA, Huang W, Venema RC, Kemp BE. Identification of regulatory sites of phosphorylation of the bovine endothelial nitric-oxide synthase at serine 617 and serine 635. *J Biol Chem*. 2001;277:42344–42351.
12. Lane P, Gross SS. Disabling a C-terminal autoinhibitory control element in endothelial nitric-oxide synthase by phosphorylation provides a molecular explanation for activation of vascular NO synthesis by diverse physiological stimuli. *J Biol Chem*. 2002;277:19087–19094.
13. Dimmeler S, Fleming I, Fisslthaler B, Hermann C, Busse R, Zeiher AM. Activation of nitric oxide synthase in endothelial cells by Akt-dependent phosphorylation. *Nature*. 1999;399:601–605.
14. Chen H, Montagnani M, Funahashi T, Shimomura I, Quon MJ. Adiponectin stimulates production of nitric oxide in vascular endothelial cells. *J Biol Chem*. 2003;278:45021–45026.
15. Harris MB, Blackstone MA, Sood SG, Li C, Goolsby JM, Venema VJ, Kemp BE, Venema RC. Acute activation and phosphorylation of endothelial nitric oxide synthase by HMG-CoA reductase inhibitors. *Am J Physiol Heart Circ Physiol*. 2004;287:560–566.
16. Chen ZP, Mitchelhill KI, Michell BJ, Stapleton D, Rodriguez-Crespo I, Witters LA, Power DA, Ortiz de Montellano PR, Kemp BE. AMP-activated protein kinase phosphorylation of endothelial NO synthase. *FEBS Lett*. 1999;443:285–289.
17. Zhang Y, Lee TS, Kolb EM, Sun K, Lu X, Sladek FM, Kassab GS, Garland T, Shyy JY. AMP-activated protein kinase is involved in endothelial NO synthase activation in response to shear stress. *Arterioscler Thromb Vasc Biol*. 2006;26:1281–1287.
18. Michell BJ, Chen ZP, Tiganis T, Stapleton D, Katsis F, Power DA, Sim AT, Kemp BE. Coordinated control of endothelial nitric-oxide synthase phosphorylation by protein kinase C and the cAMP-dependent protein kinase. *J Biol Chem*. 2001;276:17625–17628.
19. Boo YC, Hwang J, Sykes M, Michell BJ, Kemp BE, Lum H, Jo H. Shear stress stimulates phosphorylation of endothelial nitric-oxide synthase at Ser1179 by Akt-independent mechanisms: role of protein kinase A. *J Biol Chem*. 2002;277:3388–3396.

20. Fleming I, Fisslthaler B, Dimmeler S, Kemp BE, Busse R. Phosphorylation of Thr495 regulates Ca^{2+}/calmodulin-dependent endothelial nitric oxide synthase activity. *Circ Res*. 2001;88:68–75.
21. Butt E, Bernhardt M, Smolenski A, Kotsonis P, Fröhlich LG, Sickmann A, Meyer HE, Lohmann SM, Schmidt HH. Endothelial nitric-oxide synthase (type III) is activated and becomes calcium independent upon phosphorylation by cyclic nucleotide-dependent protein kinases. *J Biol Chem*. 2000;275:5179–5187.
22. Boo YC, Sorescu GP, Bauer PM, Fulton D, Kemp BE, Harrison DG, Sessa WC, Jo H. Endothelial NO synthase phosphorylated at SER635 produces NO without requiring intracellular calcium increase. *Free Radic Biol Med*. 2003;35:729–741.
23. Boo YC, Hwang J, Sykes M, Michell BJ, Kemp BE, Lum H, Jo H. Shear stress stimulates phosphorylation of eNOS at Ser(635) by a protein kinase A-dependent mechanism. Am. J. Physiol. *Heart Circ Physiol*. 2002;283:1819–1828.
24. Corton JM, Gillespie JG, Hawley SA, and Hardie DG. 5-Aminoimidazole-4-carboxamide ribonucleoside: a specific method for activating AMP-activated protein kinase in intact cells? *Eur J Biochem*. 1995;229:558–565.
25. Carling D, Clarke PR, Zammit VA, Hardie DG. Purification and characterization of the AMP-activated protein kinase. Copurification of acetyl-CoA carboxylase kinase and 3-hydroxy-3-methylglutaryl-CoA reductase kinase activities. *Eur J Biochem*. 1989;186:129–136.
26. Hardie DG. AMP-activated protein kinase as a drug target. *Annu Rev Pharmacol Toxicol.* 2007;47:185–210.
27. Levine YC, Li GK, Michel T. Agonist-modulated regulation of AMP-activated protein kinase (AMPK) in endothelial cells. Evidence for an AMPK → Rac1 → Akt → endothelial nitric-oxide synthase pathway. *J Biol Chem*. 2007;282:20351–20364.
28. Li J, Hu X, Selvakumar P, Russell RR, Cushman SW, Holman GD, Young LH. Role of the nitric oxide pathway in AMPK-mediated glucose uptake and GLUT4 translocation in heart muscle. *Am J Physiol Endocrinol Metab*. 2004;287:834–841.
29. Arad M, Seidman CE, Seidman JG. AMP-activated protein kinase in the heart: role during health and disease. *Circ Res*. 2007;100:474–488.
30. Sun W, Lee TS, Zhu M, Gu C, Wang Y, Zhu Y, Shyy JY. Statins activate AMP-activated protein kinase in vitro and in vivo. *Circulation*. 2006;114:2655–2662.
31. Calvert JW, Gundewar S, Jha S, Greer JJ, Bestermann WH, Tian R, Lefer DJ. Acute metformin therapy confers cardioprotection against myocardial infarction via AMPK-eNOS-mediated signaling. *Diabetes*. 2008;57:696–705.
32. Viollet B, Andreelli F, Jørgensen SB, Perrin C, Geloen A, Flamez D, Mu J, Lenzner C, Baud O, Bennoun M, Gomas E, Nicolas G, Wojtaszewski JF, Kahn A, Carling D, Schuit FC, Birnbaum MJ, Richter EA, Burcelin R, Vaulont S. The AMP-activated protein kinase α2 catalytic subunit controls whole-body insulin sensitivity. *J Clin Invest*. 2003;111:91–98.
33. Cheng KK, Lam KS, Wang Y, Huang Y, Carling D, Wu D, Wong C, Xu A. Adiponectin-induced endothelial nitric oxide synthase activation and nitric oxide production are mediated by APPL1 in endothelial cells. *Diabetes*. 2007;56:1387–1394.
34. McCabe TJ, Fulton D, Roman LJ, Sessa WC. Enhanced electron flux and reduced calmodulin dissociation may explain "calcium-independent" eNOS activation by phosphorylation. *J Biol Chem*. 2000;275:6123–6128.
35. Davies SP, Reddy H, Caivano M, Cohen P. Specificity and mechanism of action of some commonly used protein kinase inhibitors. *Biochem J*. 2000;351:95–105.
36. Schulz E, Anter E, Zou MH, Keaney JF. Estradiol-mediated endothelial nitric oxide synthase association with heat shock protein 90 requires adenosine monophosphate-dependent protein kinase. *Circulation*. 2005;111:3473–3480.
37. Laderoute KR, Amin K, Calaoagan JM, Knapp M, Le T, Orduna J, Foretz M, Viollet B. 5′-AMP-activated protein kinase (AMPK) is induced by low-oxygen and glucose deprivation conditions found in solid-tumor microenvironments. *Mol Cell Biol*. 2006;26:5336–5347.
38. Iseli TJ, Oakhill JS, Bailey MF, Wee S, Walter M, Denderen BJ, Castelli LA, Katsis F, Witters LA, Stapleton D, Macaulay SL, Michell BJ, Kemp BE. AMP-activated protein kinase subunit interactions: beta1:gamma1 association requires beta1 Thr-263 and Tyr-267. *J Biol Chem*. 2008;283:4799–4807.
39. Weekes J, Ball KL, Caudwell FB, Hardie DG. Specificity determinants for the AMP-activated protein kinase and its plant homologue analysed using synthetic peptides. *FEBS Lett*. 1993;334:335–339.
40. Davies SP, Carling D, Hardie DG. Tissue distribution of the AMP-activated protein kinase, and lack of activation by cyclic-AMP-dependent protein kinase, studied using a specific and sensitive peptide assay. *Eur J Biochem*. 1989;186:123–128.
41. Omkumar RV, Darnay BG, Rodwell VW. Modulation of Syrian hamster 3-hydroxy-3- methylglutaryl-CoA reductase activity by phosphorylation. Role of serine 871. *J Biol Chem*. 1994;269:6810–6814.
42. Hsieh PC, Davis ME, Lisowski LK, Lee RT. Endothelial-cardiomyocyte interactions in cardiac development and repair. *Annu Rev Physiol*. 2006;68:51–66.
43. Scott JW, Ross FA, Liu JK, Hardie DG. Regulation of AMP-activated protein kinase by a pseudosubstrate sequence on the γ subunit. *EMBO J*. 2007;26:806–815.
44. Towler MC, Hardie DG. AMP-activated protein kinase in metabolic control and insulin signaling. *Circ Res*. 2007;100:328–341.

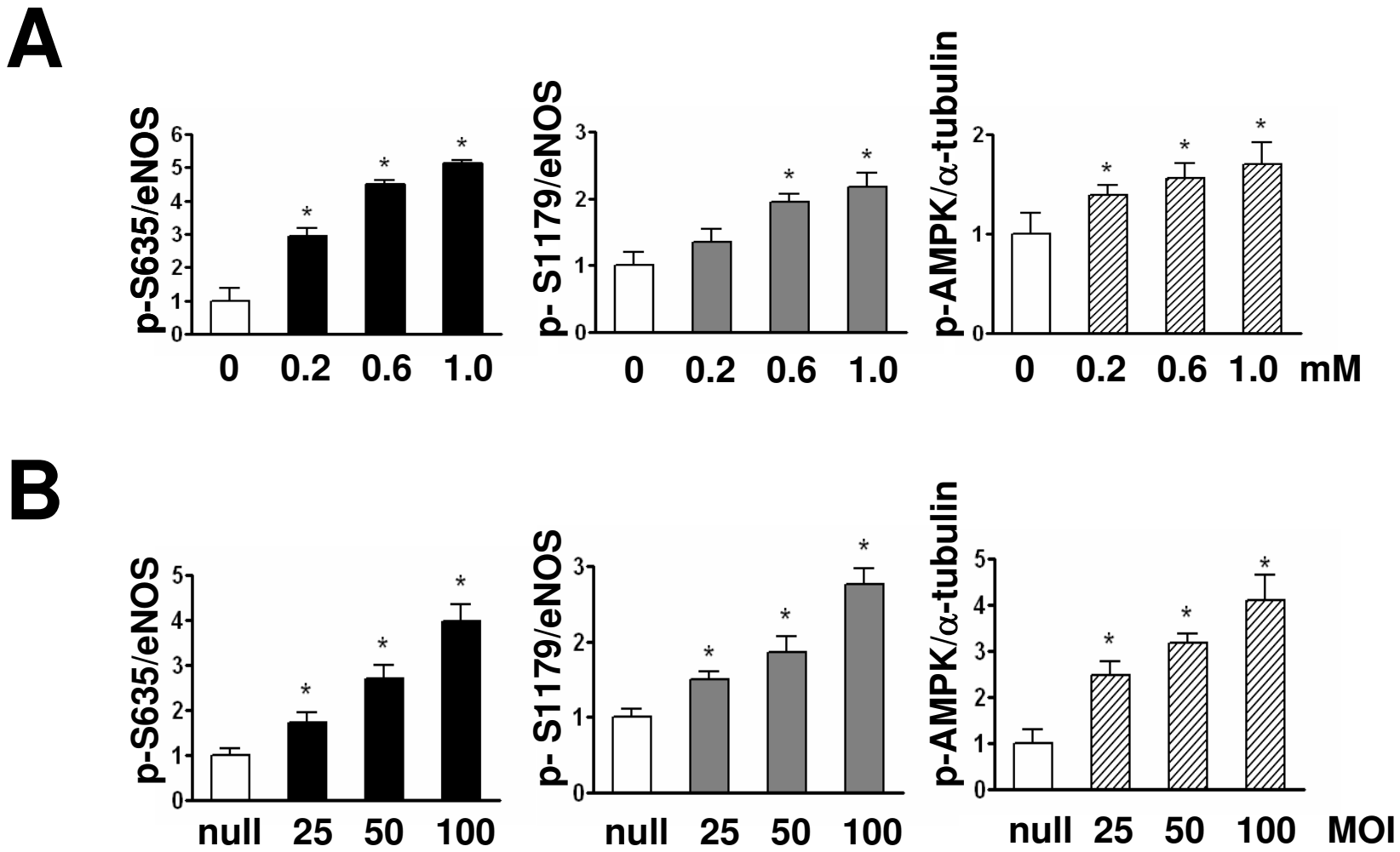

Online Figure I. Densitometry analyses of the ratios of phospho-eNOS Ser-635 or Ser-1179 to total eNOS and phospho-AMPK Thr-172 to α-tubulin examined by Western blotting in BAECs treated with various concentrations of AICAR for 15 min (A) or infected with Ad-AMPK-CA at different MOI for 24 h (B). The control cells were infected with Ad-null virus at 50 MOI. *p<0.05 between treated groups and non-treated controls.

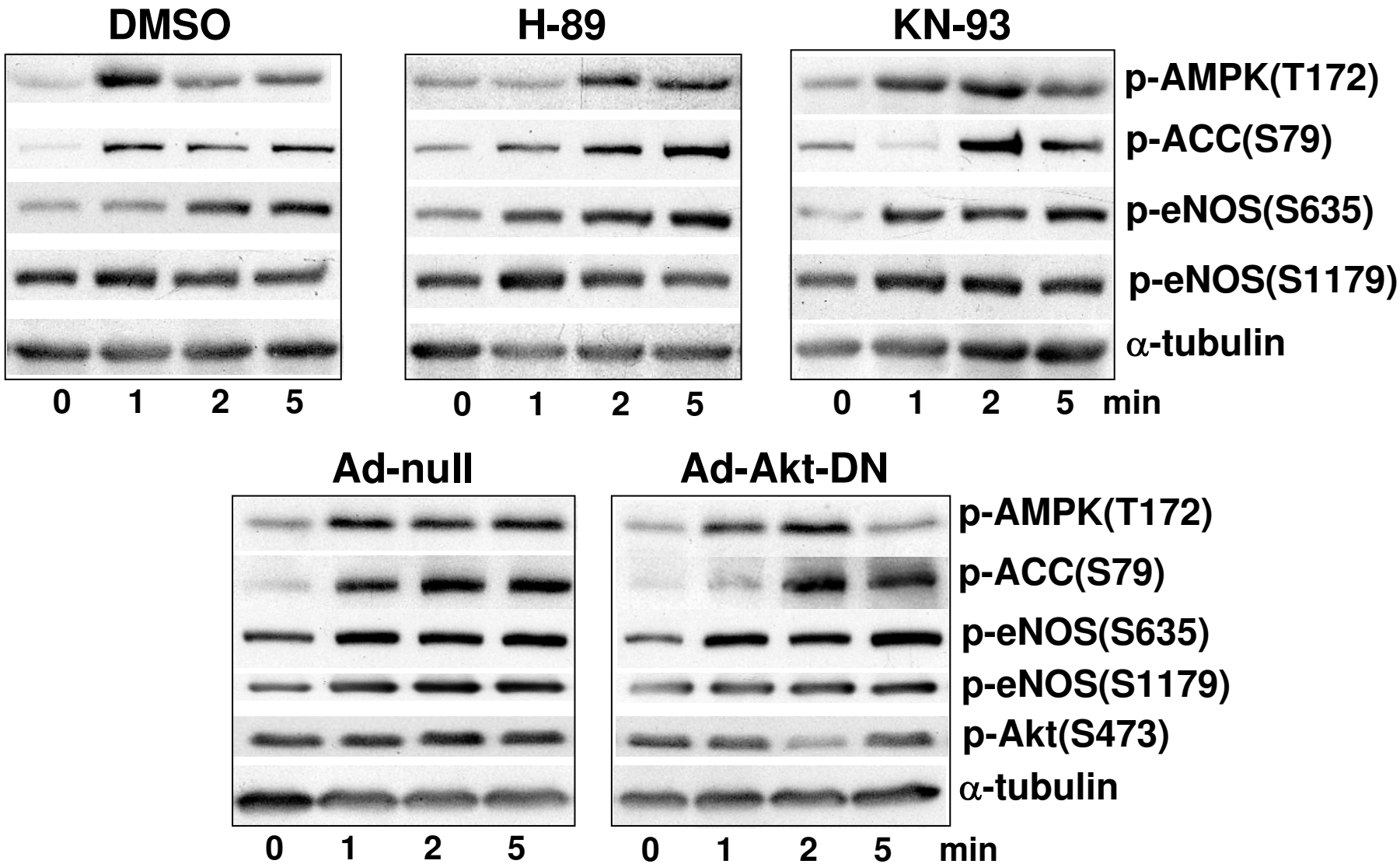

Online Figure II. BAECs were treated with H-89 (50 nM) or KN-93 (1 μM) for 30 min or infected with Ad-null control virus (50 MOI) or Ad-Akt-DN (50 MOI) expressing a dominant mutant of Akt. The cells were then subjected to a laminar shear stress at 12 dyn/cm^2 for 1, 2, and 5 min. The collected cell lysates were analyzed by Western Blot with various antibodies as indicated.

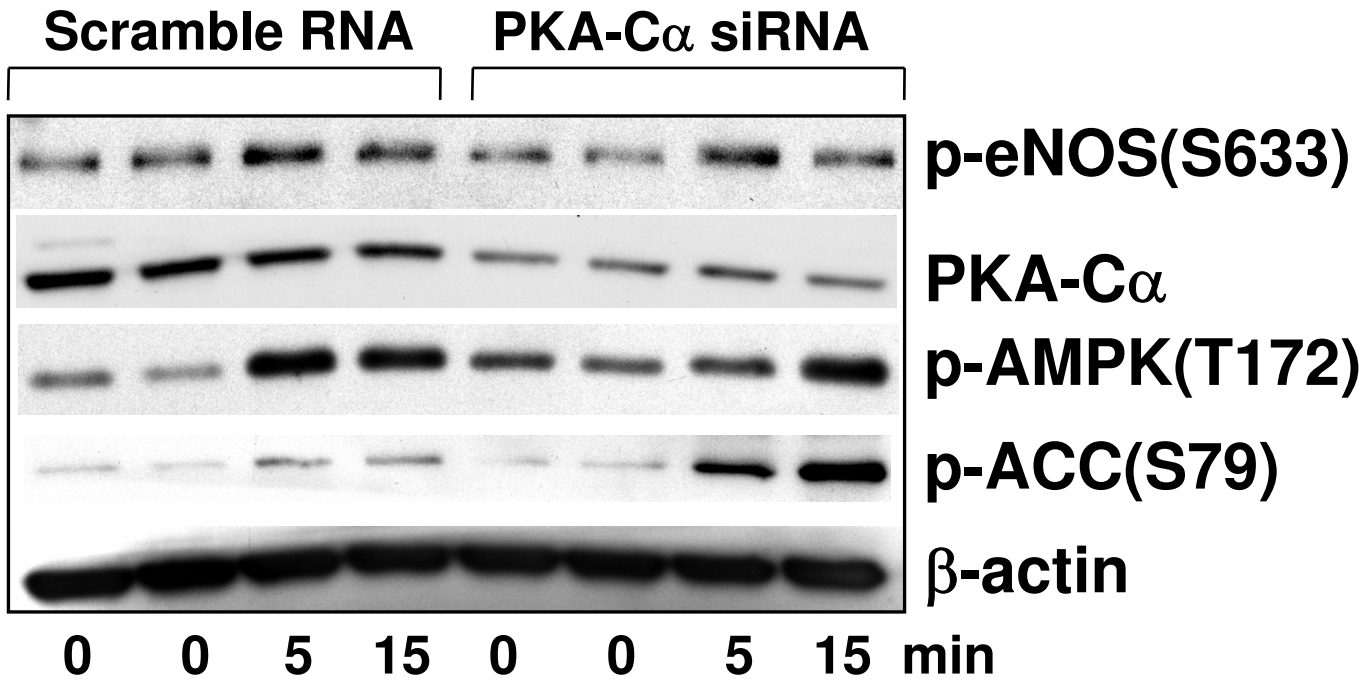

Online Figure III. HUVECs were transfected with scramble or PKACα siRNA (10 nM) against the α isofrom of the catalytic unit of PKA. Forty eight hours after transfection, the cells were subjected to laminar shear stress (12 dyne/cm^2) for 5 or 15 min. Cells kept under static condition were used as control (time 0). Cell lysates were resolved by SDS-PAGE and blotted with various antibodies as indicated.

Online Table I. The sequence, mass, and m/z for the phosphorylation of SAMS, S633, and S1177 peptides

Peptide	Sequence	Monoisotopic mass		Charge state	m/z [B]
		nonphosphorylated	phosphorylated		
SAMS	HMRSAMSGLHLVKRR[A]	1777.97	1857.93	4+	465.49
S633	PLVSSWRRKRKESSNTDSA	2203.15	2283.11	4+	571.79
S1177	RTQEVTSRIRTQSFSLQER	2321.22	2401.19	3+	801.40

[A] the putative Ser phosphorylation sites

[B] m/z, 3+ (801.40) represents phosphorylated S1177 whereas m/z 4+ (465.49 and 571.79) are those for phosphorylated SAMS and S633.

Online Supplemental Materials and Methods

Antibodies and reagents

Antibodies used were anti-pan-AMPKα, anti-AMPK-α1, anti-AMPK-α2, anti-phospho-AMPK Thr-172, anti-phospho-ACC Ser-79, anti-phospho-Akt Ser-473, anti-eNOS, and anti-α-tubulin, horseradish peroxide (HRP)-conjugated anti-rabbit or anti-mouse antibodies (Cell Signaling Technology), anti-phospho-eNOS Ser-1177/1179, and anti-phospho-eNOS Ser-633/635 (BD Biosciences Pharmingen). Griess reagent and 5-aminoimidazole-4-carboxamide 1-ribofuranoside (AICAR) were from Sigma. Compound C was from Calbiochem and atorvastatin was from Toronto Research Chemicals. Recombinant adiponectin was purchased from Phoenix Pharmaceuticals, Inc.

Cell culture, fluid shear stress experiments, adenoviral infection, and siRNA knocking down

BAECs and human embryonic kidney 293 (HEK293) cells were cultured in DMEM containing 10% FBS. MEFs were isolated from the wild-type C57BL6 or AMPKα2$^{-/-}$ mouse embryos (E13) and cultured in vitro by a standard protocol (Helgason. *Methods Mol Biol*. 2005).

The parallel-plate flow channel was used to conduct shear stress experiments (Zhang et al. *Arterioscler Thromb Vasc Biol*. 2006). BAECs were exposed to a laminar flow at 5 dyne/cm^2 for 6 h, and then the magnitude of shear stress was increased to 12 dyne/cm^2 for different time intervals.

Ad-AMPK-CA, a recombinant adenovirus expressing an AMPKα2 mutant, was described previously (Foretz et al. *Diabetes*. 2005). BAECs, HEK293 cells or MEFs

seeded on 6-well plates were infected at 70% confluency with Ad-AMPK-CA at different multiplicities of infection (MOI) and incubated for 24 h before further experimentation.

HUVECs were seeded in 6-well plates and allowed to grow to 70% confluence. Transient transfection was performed with Lipofectamine RNAiMAX. In brief, HUVECs were transfected with AMPKα1, AMPKα2 (Qiagen, SI02622235, SI02758595), or scramble siRNAs at 10 nM in reduced serum medium. Four hours after transfection, the medium was changed to fresh complete medium and cells were kept in culture for 72 h before experimentation.

Western blotting, expression of GST-eNOS proteins and IP kinase activity assays

Lysates from BAECs, HEK293 cells, MEFs, or mouse aortas were resolved on 8% SDS-PAGE, and proteins were transferred to PVDF membrane. The blotting with various antibodies followed a standard protocol as previously described (30).

The wild-type bovine eNOS cDNA in a pGEX-4T-1 vector was used as a template and the site-directed mutation at Ser-635 and Ser-1179 were performed using a QuikChange mutagenesis kit (Stratagene). Various recombinant GST-eNOS proteins were expressed in *E. Coli* and purified by glutathione 4B beads.

AMPKα was immunoprecipitated from BAEC lysates by the use of anti-pan-AMPKα. The phosphorylation of GST-eNOS by the immunoprecipitated AMPK was detected by Western blotting.

NO bioavailability assays

The bovine eNOS was subcloned into a pcDNA3 vector. The gain/loss-of-function mutants (i.e., S635A and S635D) were then created by site-directed mutagenesis

(34). Plasmids encoding pcDNA3-S635AS1179A and S635DS1179D were provided by Dr. Hanjoong Jo in Department of Biomedical Engineering, Georgia Tech and Emory University. HEK293 cells and MEFs were transiently transfected with 1 μg of respective DNA and 2.5 μl Lipofectamine 2000 (Invitrogen) per 10^6 cells. The NO production in cells transfected with various plasmids was assessed by using Griess reagent to determine the accumulated nitrite in cell culture media.

Nanoliquid chromatography/mass spectrometry

Waters' nano-Acquity UPLC (ultra performance liquid chromatography) and Q-TOF Premier mass spectrometer were used for all LC/MS and LC/MS/MS experiments. The analytical column was a BEH300 C18 column (1.7 μm particle, 75 μm internal diameter, 20 cm long) (PN# 186003544, Waters), whereas the trapping column was a Symmetry C18 column (5 μm particle, 180 μm internal diameter, 2 cm long) (PN# 186003514, Waters). Sample was loaded by the autosampler of the UPLC with a 10-μl sample loop and a partial-fill method. The LC solvents were 0.2% formic acid in water for mobile phase A and 0.2% formic acid in acetonitrile for mobile phase B. The LC gradient was as follows: 100% A at 0-3 min; 92% A/8% B at 8 min; 60%A/40% B at 70 min; 40% A/60% B at 90 min; 10% A/90% B at 100-110 min; 97% A/3% B at 115 min; 100% A at 135 min. The duration of the complete LC method was for 140 min, and LC flow rate was kept at 0.3 μl/min. A 1 hr blank injection was placed between each sample.

For SAMS and eNOS633 competition assay, SAMS was mixed with eNOS633 in ratios of 1:0, 1:1, or 1:10, and the peptide mixtures were incubated with the immunoprecipitated AMPKα in kinase assay buffer for 24 h at 37ºC. After 30 min centrifugation at 14,000 rpm, the supernatants were transferred and diluted (10x) with

0.1% trifluoroacetic acid. Three microliters of the diluted samples were analyzed by a nano-LC/MS system, which consists of Q-TOF Premier mass spectrometer, nano-Acquity UPLC (ultra-performance liquid chromatography), and a BEH130 C_{18} analytical column (Waters Corp.). Individually extracted ion chromatograms corresponding to SAMS (m/z 465.49, 4+) or eNOS633 (m/z 571.79, 4+) phosphopeptide were manually analyzed to calculate spectral intensities (ion counts) after subtraction of baseline backgrounds. The extracted ion total counts (EITC) obtained were used to quantify the changes of phosphorylation level for each peptide under the competition condition. The competition between SAMS/S1177 and S633/S1177 was analyzed in the same manner.

For eNOS phosphopeptide detection, we used the titanium dioxide (TiO_2) coated magnetic beads provided with the Phos-Trap phosphopeptide enrichment kit (PN# PRT302001KT, Perkin Elmer, Waltham, MA) to purify and enrich phosphopeptides from the trypsin-treated eNOS that was immnoprecipitated from BAECs or HEK-293 cells. eNOS was immunoprecipitated and the beads were washed twice with 1 ml of 50 mM NH_4HCO_3, pH 8.0. eNOS was then digested by adding 100 µl trypsin (20 ng/µl) directly to beads at 37ºC overnight. The buffer solutions contained in the Phos-Trap phosphopeptide enrichment kit were prepared according to manufacturer's instructions. The supernatant of trypsin-treated eNOS was lyophilized by a 4ºC speedvac concentrator and was redissolved in 20 µl trypsin buffer. The remaining beads were washed with 200 µl of the binding buffer, a component of the Phos-Trap phosphopeptide enrichment kit. After centrifugation at 14,000 rpm for 15 min, 200 µl supernantent was collected and mixed with 20 µl sample described above. Each sample was then incubated with 40 µl TiO_2-coated magnetic beads for 20 min, subjected to 4× wash with binding buffer, and

then 1× wash with washing buffer. The bound-phosphopeptides were then eluted with 30 µl elution buffer. The supernatant was collected and lyophilized. The freeze-dried pellet was dissolved in 12 µl of 0.1% trifluoro acetic acid and subjected to LC/MS/MS analyses. The phosphorylation sites within eNOS phosphopeptides were mapped by a characteristic neutral loss of the phosphate group in the process of collision-induced dissociation (CID).